

2010

A 1x2 Adaptive Optical Splitter Based on Opto-VLSI Processor.

Haithem Mustafa
Edith Cowan University

Feng Xiao
Edith Cowan University

Kamal Alameh
Edith Cowan University

[10.1109/HONET.2010.5715773](https://ro.ecu.edu.au/ecuworks/6362)

This article was originally published as: Mustafa, H. A., Xiao, F., & Alameh, K. (2010). A 1x2 Adaptive Optical Splitter Based on Opto-VLSI Processor. Proceedings of High-Capacity Optical Networks and Enabling Technologies (HONET). (pp. 200 - 203). . Cairo, Egypt. IEEE. Original article available [here](https://ro.ecu.edu.au/ecuworks/6362)

© 2010 IEEE. Personal use of this material is permitted. Permission from IEEE must be obtained for all other uses, in any current or future media, including reprinting/republishing this material for advertising or promotional purposes, creating new collective works, for resale or redistribution to servers or lists, or reuse of any copyrighted component of this work in other works.

This Conference Proceeding is posted at Research Online.

<http://ro.ecu.edu.au/ecuworks/6362>

A 1×2 Adaptive Optical Splitter Based on Opto-VLSI Processor

Haithem A. B. Mustafa, Feng Xiao, and Kamal Alameh

Electron Science Research Institute, Edith Cowan University, Australia
E-mail: hmustafa@our.ecu.edu.au

Abstract—A 1×2 adaptive optical splitter structure is proposed and experimentally demonstrated. The 1×2 adaptive optical splitter structure is based on Opto-VLSI in conjunction with 4-f imaging system. An Opto-VLSI processor is software driven and capable of splitting an optical beam into different directions when a multicasting phase hologram is uploaded. An input optical signal launched into an input optical fiber port is split and coupled into two output optical fiber ports with arbitrary splitting ratios over a wavelength range exceeding 50 nm.

Index Terms— adaptive optical splitter, beam splitter, liquid crystal devices, optical communication, opto-VLSI processor.

I. INTRODUCTION

OPTICAL power splitters mainly allow an optical line to be shared in a passive optical network (PON), (see Fig.1). The demand for optical power splitters is growing globally, due to the rapid deployment of fiber-to-the-premises (FTTP), optical metropolitan area networks (MAN), and active optical cables for TV/Video signal transport and distribution [1].

Passive optical network (PON) technology enables several hundred users to share one optical line terminal (OLT) at the central office distributing optical power to several tens of optical network units (ONUs) at the customer end of the network, each of which is shared by many users [2]. However, current PONs, which employ fixed optical power splitters, have limited reconfigurability not only to adding/dropping users to/from an ONU but also to changing services for each user.

An adaptive optical power splitter can dynamically reallocate the optical power in the entire network according to the real-time distribution of users and services, thus providing numerous advantages such as improvement of optical network efficiency and network scalability, and high network reliability. An adaptive optical power splitter is also necessary for implementing a self-healing ring in a MAN [3], which offers a popular protection mode that automatically recovers communication from failure.

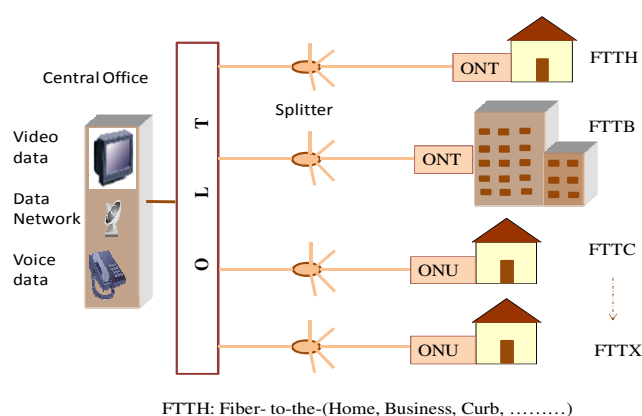


Fig. 1. Schematic architecture of a passive optical network (PON) employing 1×N passive optical splitters.

Furthermore, future optical line protection (OLP) systems require adaptive optical splitters to (i) transfer the optical power from the primary path to the secondary path dynamically, (ii) avoid the use of optical power attenuators and optical amplifiers, and (iii) monitor both paths instantaneously [4]. Moreover, adaptive optical power splitters can add many advantages into fiber CATV networks, including substantial improvement in network adaptability and scalability [5].

Currently, the majority of optical power splitters are passive [6-10]. Passive splitters based on Planar Lightwave Circuits (PLC) are low-cost, however, they do not provide network flexibility. Recently, only a few dynamic optical splitter structures have been reported [5], [11]-[14]. However, these structures have different limitation such as noisy and uncontrollable output power level, reliability, and tolerance to environmental perturbations (temperature, vibrations, etc).

In this paper, we propose and experimentally demonstrate the concept of a new adaptive optical splitter structure based on the use of an Opto-VLSI processor in conjunction with a 4-f imaging system. This adaptive optical splitter can be reconfigured via software to provide arbitrary optical power splitting profiles/ratios for multiple output channels. In addition,

the adaptive optical splitter has attractive features, such as a simple architecture, ability to synthesize arbitrary and accurate power splitting ratios, low power loss, and easy user interface.

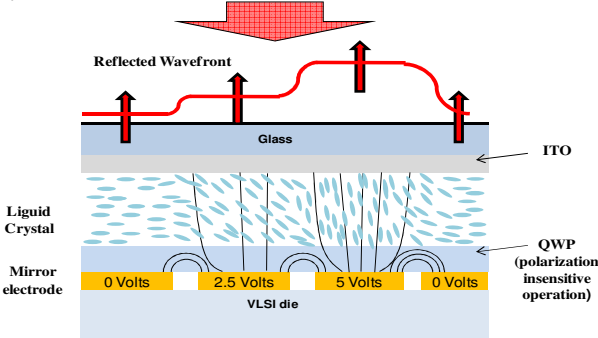


Fig. 2. Opto-VLSI processor layout, Opto-VLSI cell structure and pixel architecture.

II. OPTO-VLSI PROCESSORS AND OPTICAL BEAM MULTICASTING

The Opto-VLSI processor is a diffraction element capable of steering/shaping an incident optical beam electronically without mechanically moving parts. As shown in Fig. 2, an Opto-VLSI processor comprises an array of liquid crystal (LC) cells driven by a Very-Large-Scale-Integrated (VLSI) circuit [14, 15], which generates digital holographic diffraction gratings that achieve arbitrary beam deflection/multicasting. A transparent Indium-Tin Oxide (ITO) layer is used as the second electrode, and a quarter-wave-plate (QWP) layer is deposited between the LC and the aluminum mirror to accomplish polarization-insensitive operation. The voltage level of each pixel can individually be controlled by using a few memory elements that select a discrete voltage level and apply it, through the electrodes, across the LC cell.

A multicasting phase hologram can split an incident optical beam to N output beams with variable intensities in different directions, as illustrated in Fig. 3. A collimated beam incident onto the Opto-VLSI processor is diffracted along different directions, where the power of each diffracted beam depends on the multicasting phase hologram. The beam multicasting resolution, or minimum splitting angle relative to the zeroth order diffraction beam, is given by [16]

$$\alpha = \arcsin\left(\frac{\lambda}{N \times d}\right) \quad (1)$$

where λ is the optical wavelength, N denotes the number of pixels illuminated by the incident optical beam, and d is the pixel pitch. Several computer algorithms, such as the genetic, simulated annealing, phase encoding, and projection algorithms [17], have been used for generating optimized multicasting phase holograms that

produce a target far-field distribution, defined by the replay beam positions and the corresponding power splitting ratios.

For a target optical splitting ratio profile, an optimised phase hologram can always be generated, which minimizes the power of the zeroth order diffraction beam and maximizes the signal-to-crosstalk ratio at every output port.

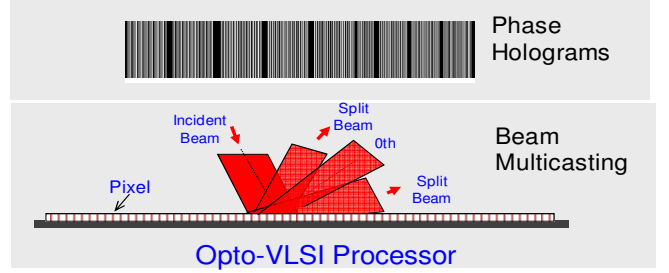


Fig. 3. Illustration of the optical beam multicasting capability of an Opto-VLSI processor by uploading phased holograms.

III. EXPERIMENTS

A. System description

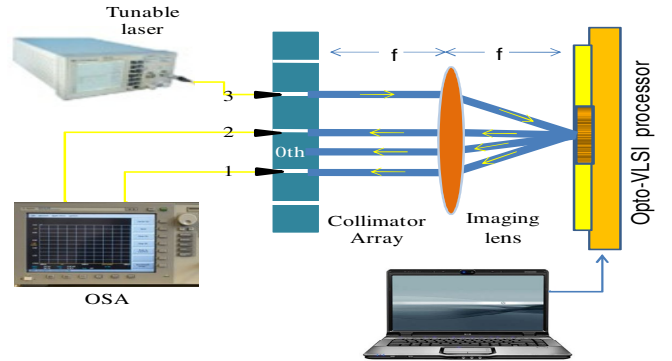


Fig. 4. Schematic diagram of the proposed adaptive optical splitter using an Opto-VLSI processor and a 4-f imaging systems.

The structure of the proposed adaptive optical power splitter is shown in Fig. 4, through an experimental setup. It consists of an Opto-VLSI processor, a lens, and an optical fiber collimator array, aligned to form a 4-f imaging system. The Opto-VLSI processor has 1×4096 pixels with pixel size of $1.0 \mu\text{m}$ wide and 6.0mm length, and $1.8 \mu\text{m}$ pixel pitch (i.e. $0.8 \mu\text{m}$ of dead space between pixels).

To prove the concept of adaptive optical splitting, only three ports of the fiber collimator were used, thus demonstrating a 1×2 adaptive optical power splitter. A 1550nm laser source of $+5 \text{dBm}$ optical power was used as an input signal, and launched through Port 3 of the fiber collimator array. Port 1 and Port 2 were used as the output ports. The spacing (C) between the fiber

collimator elements was 3 mm. A lens of focal length $f = 100$ mm was placed between and at an equal distance, f , from both the fiber collimator array and the Opto-VLSI processor. With no phase hologram uploaded onto the Opto-VLSI processor, only the 0th order diffraction beam was reflected back and focused through the imaging system onto a spot in between the fiber collimator ports, resulting in minimum crosstalk coupled into ports 1 and 2, as illustrated in Fig. 4. The beam diameter at the fiber collimator was 1 mm. The beam propagated through a lens, which focused it to 0.8 mm at the Opto-VLSI processor, thus illuminating around 440 pixels.

By driving the Opto-VLSI processor with an optimized multicasting phase hologram, the optical beam illuminating the Opto-VLSI processor was split into two different optical beams (in addition to the 0th order beam) which propagated along the optimized directions so that they were respectively coupled back into Port 1 and 2 of the fiber collimator through the 4-f imaging system. The split optical beams coupled into the two output ports propagated along angles equal to $\theta = \pm \arctan(C/2f) \approx \pm 0.86^\circ$ with respect to the 0th order diffraction beam. Two optical spectrum analyzers (OSA) were used to monitor the power levels of the split optical signals coupled into the two output ports.

Note that a fiber collimator array, rather than a fiber array, was used in this experiment in order to avoid stringent alignment conditions, such as the use of highly accurate optical stages, to maximize the optical power coupled into the output ports. Note also that the diameter of the focused optical beam at the Opto-VLSI processor was relatively large (in order to illuminate a large number of pixels) leading to a high diffraction efficiency and high optical splitting resolution as described in Eq. (1). This 4-f imaging system enabled adaptive optical splitting with large tolerance to misalignment to be achieved.

B. Experimental Results and Discussion

Several optical splitting ratios and profiles were attempted in the experiments to demonstrate the adaptive optical power splitting capability of the proposed optical splitter. Fig. 5 shows the measured output power levels, P_1 and P_2 , at Port 1 and Port 2, respectively, corresponding to different splitting ratios.

For a splitting ratio equal to zero (i.e. $P_1=0$), as shown Fig. 5(a), the input optical signal was steered to Port 2, through a steering phase hologram, resulting in a very small optical signal power being measured at Port 1. The optical splitting ratio can continuously be changed from 0.021 (-16.6 dB) to around 50 (17 dB).

When the optical splitting ratio was changed to 1.0 (i.e. splitting the input power equally to the two output ports), the measured output power levels at Port 1 and Port 2 were 307 μ W and 305 μ W, respectively, as illustrated in Fig. 5(b).

Fig. 6 shows the optical power ratio of the measured optical power at the two output fiber ports versus the targeted splitting ratio, and demonstrates the ability of the adaptive splitter structure to realize arbitrary optical splitting ratios. Excellent agreement between the measured optical power ratio of the two output ports and the target optical splitting ratio, demonstrating that the total output power ($P_{\text{tot}} = P_1 + P_2$) split into Port 1 and Port 2 remains invariable every time a new optimized multicasting phase hologram is uploaded onto the Opto-VLSI processor for realizing a target optical splitting ratio.

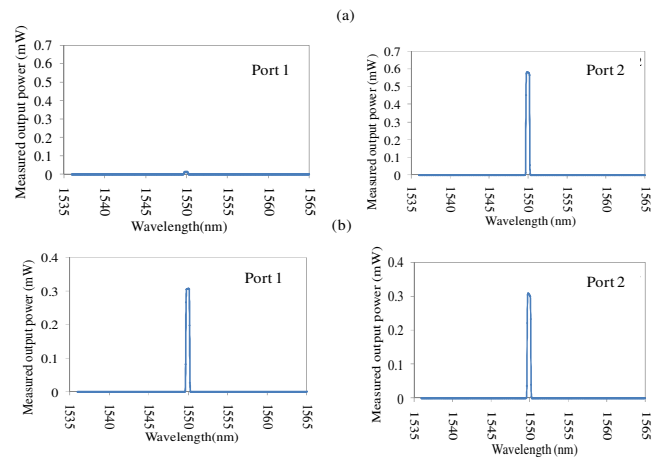


Fig. 5. Measured output power at Port 1 and Port 2 (i.e., P_1 and P_2) for different splitting ratios. (a) Splitting ratio $P_1/P_2=0$, and (b) $P_1/P_2=1$.

To investigate the bandwidth of the proposed adaptive optical splitter, a tunable laser source of wavelength range from 1525nm to 1575nm was used at the input fiber port. The measured output power at ports 1 and 2 versus wavelength are shown in Fig. 7, for an optical splitting ratio equal to 1.0. The measured maximum output power fluctuation at the two output ports was less than 0.1 dB over a wavelength span from 1525 to 1575 nm, demonstrating a splitter bandwidth in excess of 50 nm.

The total insertion loss of the optical power splitter was about 5 dB, to which the Opto-VLSI processor contributed around 3dB due to its low fill factor. The beam steering loss was 0.5 dB and the fiber collimator array in conjunction with the lens contributed the remaining 1.5 dB of insertion loss. However, the total insertion loss can be reduced through (i) an improved Opto-VLSI chip design, where the dead-space between pixels is reduced to below 0.25 micron, and (ii) the use

of broadband AR coatings for the various optical components.

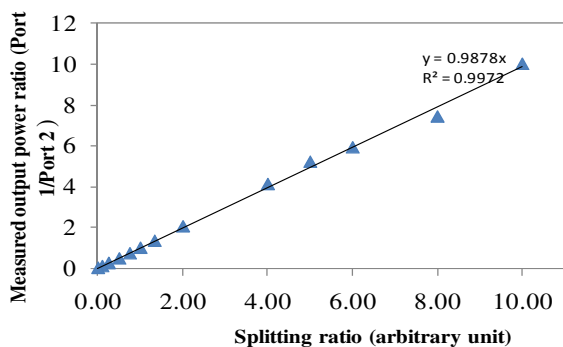


Fig. 6. Measured output powers at (Port1/Port 2) versus the targeted splitting ratio (P_1/P_2).

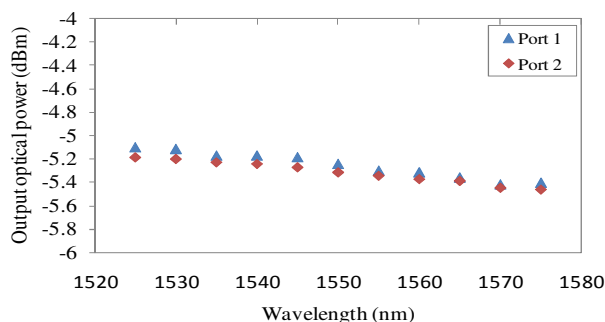


Fig. 7. Measured output power at ports 1 and 2 versus wavelength for a splitting ratio = 1.0.

The total insertion loss of the adaptive optical power splitter was relatively large for a 1×2 optical splitter. However, this optical splitter structure has the potential to realize a large number of output ports with negligible insertion loss penalty. The latter feature makes the proposed splitter attractive for many emerging optical network applications, in comparison to other adaptive optical power splitters that have a limited number of output ports.

Note that the large spacing between the elements of the collimator array used in this experiment resulted in a limited number of output ports. However, by reducing the spacing between the fiber collimator elements to around 1 mm, more than 10 output ports can be achieved. Furthermore, by using a 2-dimensional Opto-VLSI processor and a 2-dimensional optical fiber collimator array, a high-resolution dynamic optical splitter with up to 100 output ports can potentially be realized.

IV. CONCLUSION

A 1×2 adaptive optical splitter structure based on the use of an Opto-VLSI processor in conjunction with a 4-f imaging system has been proposed and experimentally

demonstrated. Experimental results have demonstrated that an input optical signal can arbitrarily be split into two signals and coupled into optical fiber ports by uploading optimized multicasting phase holograms onto the Opto-VLSI processor. A bandwidth exceeding 50 nm over the C-band of optical telecommunications has been measured, making the adaptive splitter attractive for many optical network applications.

REFERENCES

- [1] G. A. Queller, "Dynamic power distribution in PON/FTTP networks," *Lightwave* vol. 21, no. 7, 2004 [Online]. Available: <http://www.lightwaveonline.com/about-us/lightwave-issue-archives/issue/dynamic-power-distribution-in-ponfttp-networks-53906787.html>
- [2] M. D. Vaughn, D. Koziscek, D. Meis, A. Boskovic, and R. E. Wagner, "Value of reach-and-split ratio increase in FTTH access networks," *J. Lightw. Technol.*, vol. 22, no. 11, pp. 2617–2622, Nov. 2004.
- [3] J. Shi and J. P. Fonseka, "Hierarchical self-healing rings," *IEEE/ACM Trans. Netw.*, vol. 3, no. 6, pp. 690–697, Dec. 1995.
- [4] D. Griffith and S. Lee, "A $1 + 1$ protection architecture for optical burst switched networks," *IEEE J. Sel. Areas Commun.*, vol. 21, no. 9, pp. 1384–1398, Nov. 2003.
- [5] Z. Yun, L. Wen, C. Long, L. Yong, and X. Qingming, "A 1×2 variable optical splitter development," *J. Lightw. Technol.*, vol. 24, no. 3, pp. 1566–1570, Mar. 2006.
- [6] T. J. Wang, C. F. Huang, and W. S. Wang, "Wide-angle 1×3 optical power divider in LiNbO₃ for variable power splitting," *IEEE Photon. Technol. Lett.*, vol. 15, no. 10, pp. 1401–1403, Oct. 2003.
- [7] K. B. Chung and J. S. Yoon, "Properties of a 1×4 optical power splitter made of photonic crystal waveguides," *Opt. Quantum Electron.*, vol. 35, pp. 959–966, 2003.
- [8] A. Ghaffari, M. D. Javid, and M. S. Abrishman, "Power splitters with different output power levels based on directional coupling," *Appl. Opt.*, vol. 48, no. 8, pp. 1606–1609, 2009.
- [9] I. Park, H. S. Lee, H. J. Kim, K. M. Moon, S. G. Lee, B. H. O, S. G. Park, and E. H. Lee, "Photonics crystal power-splitter based on directional coupling," *Opt. Exp.*, vol. 12, no. 15, pp. 3599–3604, 2004.
- [10] Y. Zhang, L. Liu, X. Wu, and L. Xu, "Splitting-on-demand optical power splitters using multimode interference (MMI) waveguide with programmed modulations," *Opt. Commun.*, vol. 281, pp. 426–432, 2008.
- [11] F. Ratovelomanana, N. Vodjdani, A. Enard, G. Glasere, D. Rondi, and R. Blondeau, "Active lossless monolithic one-by-four splitters/combiners using optical gates on InP," *IEEE Photon. Technol. Lett.*, vol. 7, no. 5, pp. 511–513, May 1995.
- [12] S. S. Choi, J. P. Donnelly, S. H. Groves, R. E. Reeder, R. J. Bailey, P. J. Taylor, A. Napoleone, and W. D. Goodhue, "All-active In- GaAsP-InP optical tapered-amplifier $1 \times N$ power splitters," *IEEE Photon. Technol. Lett.*, vol. 12, no. 8, pp. 974–976, Aug. 2000.
- [13] X. Zhao and S. Jose, "Dynamic Power Optical Splitter," U.S. Patent 7 068 939 B2, Jun. 27, 2006.
- [14] R. Zheng, Z. Wang, K. E. Alameh, and W. A. Crossland, "An opto-VLSI reconfigurable broadband optical splitter," *IEEE Photon. Technol. Lett.*, vol. 17, no. 2, pp. 339–341, Feb. 2000.
- [15] F. Xiao, B. Juswardy, and K. Alameh, "Novel broadband reconfigurable optical add-drop multiplexer employing custom fiber arrays and opto-VLSI processors," *Opt. Exp.*, vol. 16, no. 16, pp. 11703–11708, 2008.
- [16] F. Xiao, K. Alameh, and T. T. Lee, "Opto-VLSI-based tunable single mode fiber," *Opt. Exp.*, vol. 17, no. 21, pp. 18676–18680, 2009.
- [17] S. T. Ahderom, M. Raisi, K. Alameh, and K. Eshraghian, "Testing and analysis of computer generated holograms for microphotonic devices," in *Proc. 2nd IEEE Int. Workshop Electron. Design, Test Appl. (DELTA)*, Australia, 2004, pp. 47–52.